Theor Appl Climatol (2011) 106:343–354
DOI 10.1007/s00704-011-0436-6

ORIGINAL PAPER

# A modeling study of the effects of aerosols on clouds and precipitation over East Asia

**Xiaodong Liu · Xiaoning Xie · Zhi-Yong Yin · Changhai Liu · Andrew Gettelman**

Received: 18 January 2011 / Accepted: 17 March 2011 / Published online: 14 April 2011


**Abstract** The National Center for Atmospheric Research Community Atmosphere Model (version 3.5) coupled with the Morrison–Gettelman two-moment cloud microphysics scheme is employed to simulate the aerosol effects on clouds and precipitation in two numerical experiments, one representing present-day conditions (year 2000) and the other the pre-industrial conditions (year 1750) over East Asia by considering both direct and indirect aerosol effects. To isolate the aerosol effects, we used the same set of boundary conditions and only altered the aerosol emissions in both experiments. The simulated results show that the cloud microphysical properties are markedly affected by the increase in aerosols, especially for the column cloud droplet number concentration (DNC), liquid water path (LWP), and the cloud droplet effective radius (DER). With increased aerosols, DNC and LWP have been increased by 137% and 28%, respectively, while DER is reduced by 20%. Precipitation rates in East Asia and East China are reduced by 5.8% and 13%, respectively, by both the aerosol's second indirect effect and the radiative forcing that enhanced atmospheric stability associated with the aerosol direct and first indirect effects. The significant reduction in summer precipitation in East Asia is also consistent with the weakening of the East Asian summer monsoon, resulting from the decreasing thermodynamic contrast between the Asian landmass and the surrounding oceans induced by the aerosol's radiative effects. The increase in aerosols reduces the surface net shortwave radiative flux over the East Asia landmass, which leads to the reduction of the land surface temperature. With minimal changes in the sea surface temperature, hence, the weakening of the East Asian summer monsoon further enhances the reduction of summer precipitation over East Asia.

X. Liu (✉) · X. Xie · Z.-Y. Yin
SKLLQG, Institute of Earth Environment,
Chinese Academy of Sciences,
Xi'an 710075, China
e-mail: liuxd@loess.llqg.ac.cn

C. Liu · A. Gettelman
National Center for Atmospheric Research,
PO Box 3000, Boulder, CO 80307, USA

Z.-Y. Yin
University of San Diego,
San Diego, CA 92110, USA

## 1 Introduction

Atmospheric aerosols, as a fundamental but variable ingredient of atmosphere, can affect climate remarkably. Atmospheric aerosols influence global and regional climate directly by scattering and absorbing incoming solar radiation (the aerosol direct effect), and act as cloud condensation nuclei and ice nuclei to modify the cloud radiative properties indirectly (the first aerosol indirect effect, Twomey 1974), and the onset and amount of precipitation (the second aerosol indirect effect, Albrecht 1989). Aerosol's direct and indirect effects can modify the atmospheric temperature structure, which may affect convection and monsoonal circulations and further alter the hydrological cycle in a region (Ramanathan et al. 2001; Rosenfeld et al. 2008).

The climatic effects of aerosols have long been recognized, but the tasks to quantify these effects in the context of climate change are extremely difficult due to the complexity of the physical processes and lack of observations. The Intergovernmental Panel on Climate Change (IPCC 2007) summarized the progress in aerosol studies since the late 1990s and emphasized the advances in

satellite-based retrieval of atmospheric aerosol concentration that filled the gaps of ground-based observations. However, this does not change the fact of the lack of long-term observational data with sufficient spatial coverage to fully explore the spatial and temporal variation patterns of atmospheric aerosols. This is also the reason why model simulations have become an important means in the studies of the climatic effects of aerosols. To facilitate improvements of the models, the Global Aerosol Model Intercomparison (AeroCom) initiative was conducted (Kinne et al. 2006), with participation of 16 modeling groups, including the CCM3, the earlier version of the National Center for Atmospheric Research (NCAR)'s Community Climate System Model (Kiehl and Gent 2004).

In the past few decades, with rapid population growth and economic development, Asia, the world's most densely populated continent, has become a major source of aerosol emissions (Remer et al. 2008; Massie et al. 2004). Furthermore, many studies indicate that the increase in aerosols plays an important role in the change of the Asian summer monsoon intensity and precipitation regimes. For example, atmospheric brown clouds mainly induced by biomass burning and fossil fuel consumption can affect the South Asia climate and hydrological cycle (Ramanathan et al. 2005), which also enhances the warming trends of the high altitude region of the Himalayas (Ramanathan et al. 2007). Some researchers suggest that the "elevated heat pump" induced by the warm air over the Tibetan Plateau heated by the absorptive aerosols including dust and black carbon can affect the annual evolution of the Asia summer monsoon circulation, which leads to an earlier occurrence of the monsoon rainy season and subsequently an intensification of the Indian summer monsoon (Lau et al. 2006; Lau and Kim 2006).

In China, located in East Asia, the main characteristic of precipitation is the dominance of the Asian summer monsoon system. Previous studies have found a drying trend in the north, which coincides with a wetting trend in the central eastern part of China, forming a spatial pattern of "north drought with south flooding" since the 1970s (Xu 2001; Hu et al. 2003). Several mechanisms have been proposed to explain this pattern. For example, it has been suggested that these changes are closely related to the large-scale atmospheric circulation anomalies and the weakening Asian summer monsoon (Xu 2001; Hu et al. 2003). Menon et al. (2002) used a global climate model to investigate possible aerosol contributions from India and China to the changes in precipitation across the East Asia monsoon region, and found that the increased rainfall in the middle and lower reaches of the Yangtze River and droughts in North China may be related to increased black carbon aerosols. However, several subsequent studies (Gu et al. 2006; Meehl et al. 2008; Zhang et al. 2009) do not fully support the findings by Menon et al. (2002).

The causes of the enhanced drought conditions in the region from the eastern part of Northwest to North China in the last few decades are complex. For example, a shift from the wet to dry condition in this region around the mid- to late-1970s may be related to the regional response to global warming (Fu and Ma 2008), the phase change of the Pacific Decadal Oscillation (Ma 2007), or the interannual variability of the snow cover over the Tibetan Plateau (Ding et al. 2009). It is also possible that that the reduced precipitation and increased droughts in North China have been caused by the increase in aerosol concentrations. Zhao et al. (2006) analyzed the observed precipitation data, aerosol optical depth (AOD) retrieved from satellite data (MODIS), and conventional meteorological sounding data over eastern China, and found that there might be various feedback mechanisms between the reduced precipitation in this region during the last 40 years and the high concentrations of anthropogenic aerosols. Based on historical data of precipitation and visibility for North China, Duan and Mao (2009) indicated that anthropogenic aerosols in North China can reduce local precipitation. Several simulation results (Menon et al. 2002; Giorgi et al. 2003; Huang et al. 2007) also pointed to aerosols as a factor that can lead to the cooling of land surface in North China and further decrease precipitation. However, Qian et al. (2009) claimed that the increasing aerosols could only suppress light rain in East China; while other simulation results showed that the effects of aerosols on precipitation over China are not evident (e.g., Qian et al. 2003) and the effects of aerosol absorption can even increase atmospheric vapor content and precipitation in northern and northwestern China (Wu et al. 2009).

Overall, parts of East Asia, especially North China, in recent years have experienced a significant drying trend, and the increase in atmosphere aerosols could be one of the reasons of such changes. However, from the above discussion, we can see that there are different opinions on the scope, extent, and mechanisms of aerosol's effects on precipitation over East China. Most of the previous simulation studies have mainly focused on the changes in precipitation induced by the aerosol's direct radiative forcing effect, with much less attention paid to the aerosol's indirect effects (acting as cloud condensation nuclei or ice nuclei). Additionally, the simulation studies of the indirect effects of aerosols tend to be less conclusive with large ranges of uncertainties due to the complexity of the physical processes (IPCC 2007). Much work is still needed for us to improve our understanding of the climatic effects of aerosols, especially in East Asia where dramatic increases in anthropogenic aerosol emissions have occurred. In this study, we will use the latest version of the

NCAR Community Atmosphere Model (CAM; version 3.5) coupled with the Morrison–Gettelman two-moment cloud microphysics scheme (Morrison and Gettelman 2008) to simulate the aerosol effects on clouds and precipitation for the present-day condition in comparison with the pre-industrial condition over East Asia, especially for the heavily polluted East China, with considerations of both the direct and indirect effects of the aerosols to achieve a more complete understanding of the climatic effects of the aerosols.

## 2 Model description and experimental design

The CAM version 3.5 is developed by NCAR (Gent et al. 2009), as the improved version of CAM 3.0 (Collins et al. 2004). The model is normally run for a 5-year time period with 2.5° (longitude)×1.9° (latitude) horizontal resolution and 26 vertical levels. The modifications in the new version include the new two-moment microphysics scheme (Morrison and Gettelman 2008; Gettelman and Morrison 2008) including the autoconversion parameterization from Khairoutdinov and Kogan (2000), which predicts the mass mixing ratio and the number concentration of five hydrometeor species: cloud droplets, rain drops, ice crystals, snow, and graupel, and feeds the results into the radiative forcing module. The Morrison–Gettelman scheme considers the indirect aerosol effects (including both the aerosol's first indirect and second indirect effects); however in this scheme, the aerosols only act as cloud condensation nuclei in warm clouds, not as ice nuclei. A global 3-D chemical transport model, the model for ozone and related chemical tracers (MOZART) Bulk Aerosol Model (Emmons et al. 2010) is interactively coupled in CAM 3.5 with 13 bins of aerosols: four bins of dust, four bins of sea salt, one bin of sulfate, two bins of black carbon, and two bins of organic carbon. The meteorological fields used in MOZART are taken from online calculations in the CAM model, and the distributions of aerosols used in CAM come from the subsequent output of MOZART.

Following the AeroCom scheme (Quaas et al. 2009) we designed two experiments, with one representing the present-day condition (PD) in year 2000 and the other for the pre-industrial condition (PI) in year 1750. In simulation, we use the averages of the last 5 years for the comparison between the two experiments, often presented as the present-day–pre-industrial differences (PD–PI). The sources of the aerosol emissions for both the year 1750 and 2000 are prescribed from the AeroCom emissions datasets (Dentener et al. 2006). Then we analyze the simulated results of aerosol emissions and the state of climate of the years 2000 and 1750. Except for the aerosol emissions, all boundary conditions of the simulations are kept the same in the PD and PI experiments in order to isolate the aerosol effects. For example, model input variables, such as the greenhouse gas concentrations and sea surface temperature (SST), are all from estimates of the present-day condition. We would like to note that the global simulation results of the CAM 3.5 with the Morrison–Gettleman two-moment scheme have been used in the most recent round of AeroCom intercomparison and model evaluation based on satellite data (Quaas et al. 2009). In this study, we emphasize the responses of the state of climate and simulation results regarding clouds and precipitation properties over East Asia and, especially, East China induced specifically by the changes in aerosol emissions. Unless otherwise noted, East Asia is designated as the region 77.5–162.5°E and 18–61.6°N, and East China as 100–122.5°E and 25.6–42.6°N in the following.

## 3 Results

### 3.1 Precipitation change due to aerosol increases

The aim of our study is to investigate the possible changes in precipitation regimes caused by atmospheric aerosols over East Asia and East China. We use the AOD as the measure of regional characteristics of aerosol emissions. Obviously, the simulated AOD of the PD experiment is much higher than the simulated AOD of the PI experiment. Figure 1 shows the spatial distribution patterns of the seasonal (spring, MAM; summer, JJA; fall, SON; and winter, DJF) and annual PD–PI AOD differences. It can be seen that AOD increases markedly over East Asia in PD from the PI levels, while the spatial patterns of the changes in AOD are similar in all seasons, with the largest increases mainly in the region from the lower reach of the Yangtze River to North China in eastern China. The increases in spring and summer are higher than those in the other seasons (up to 0.7 and higher) and the region with large increases (>0.6) tends to shift and expand toward northeast from spring to summer, eventually encompassing almost the entire East Asia from central eastern China to Korea and Japan. The PD–PI AOD difference in winter is much smaller and the increases occur mainly in southern China. Since dramatic changes have happened in the amount and spatial pattern of precipitation in East China, as we described earlier, which coincide with the enhanced aerosol emissions in the region in recent decades, we want to first analyze the results of the numerical experiments to examine the effects of aerosols on clouds and precipitation in East Asia, especially in East China.

Figure 2a shows the simulated field of annual mean precipitation rate over East Asia (77.5–162.5°E, 18–61.6°N) in the PD experiment. Except for a high precipi-

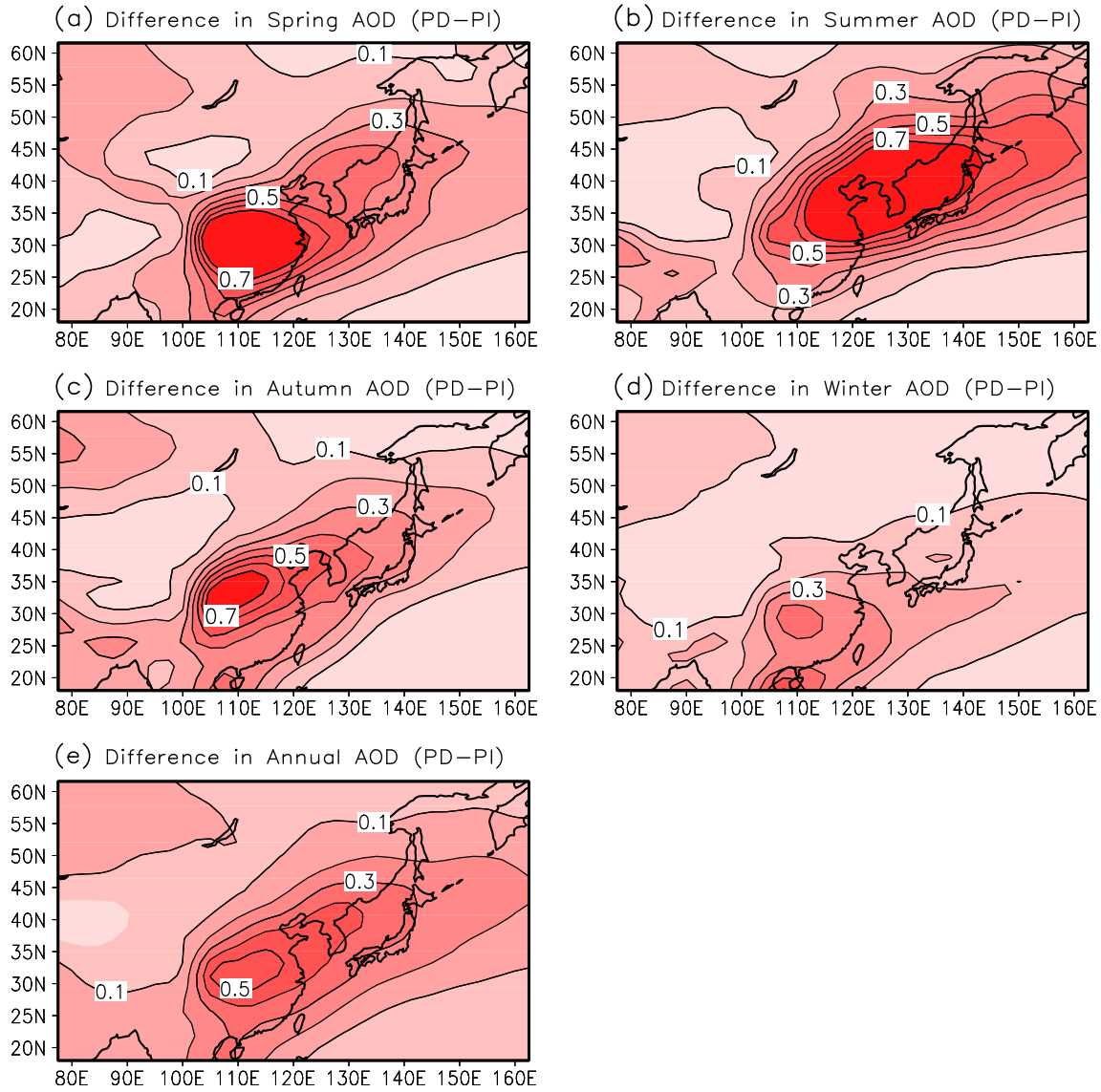


**Fig. 1** Spatial distributions of AOD differences between the PD and PI experiments for spring (March–May, **a**), summer (June–August, **b**), autumn (September–November, **c**), winter (December–February, **d**), and annual (**e**) averages

tation area south of the Himalayas, there is a general decreasing trend in the spatial distribution of precipitation rate from the southeastern coast to the northwest, which is the same as the observed pattern. The magnitude of the precipitation rates is normally 2–4 mm/day in East China, while those in the inland arid regions are often less than 1 mm/day. Figure 2b displays the changes in the simulated annual mean precipitation rates (as PD–PI). Since we use the same set of boundary conditions in the simulation, the differences between the two experiments are entirely caused by the changes in the aerosol emissions. Apparently, the increases in aerosols have lead to a significant reduction in the simulated precipitation in the East Asian low-middle latitude region, especially in East China (100–122.5° E, 25.6–42.6° N). The reductions of precipitation are presented not only in large-scale precipitation (Fig. 2d) but also in convective precipitation (Fig. 2f). The average annual mean precipitation rate of East Asia has reduced from 3.09 mm/day in PI to 2.92 mm/day in PD, a reduction of 5.8% (Table 1). From the seasonal perspective, the reduction in the summer precipitation rate is largest (9.5%) although a similar reduction is seen in spring. Moreover, the changes in large-scale precipitation (−9.3%) and those in convective precipitation (−9.5%) have made nearly the same contributions to the decreased total precipitation in summer. There is a much smaller reduction in fall, while the precipitation rate actually increases slightly in winter. The reason for the increase in winter precipitation, exclusively in the form of large-scale precipitation, however, remains unclear at present. Though several simulation studies

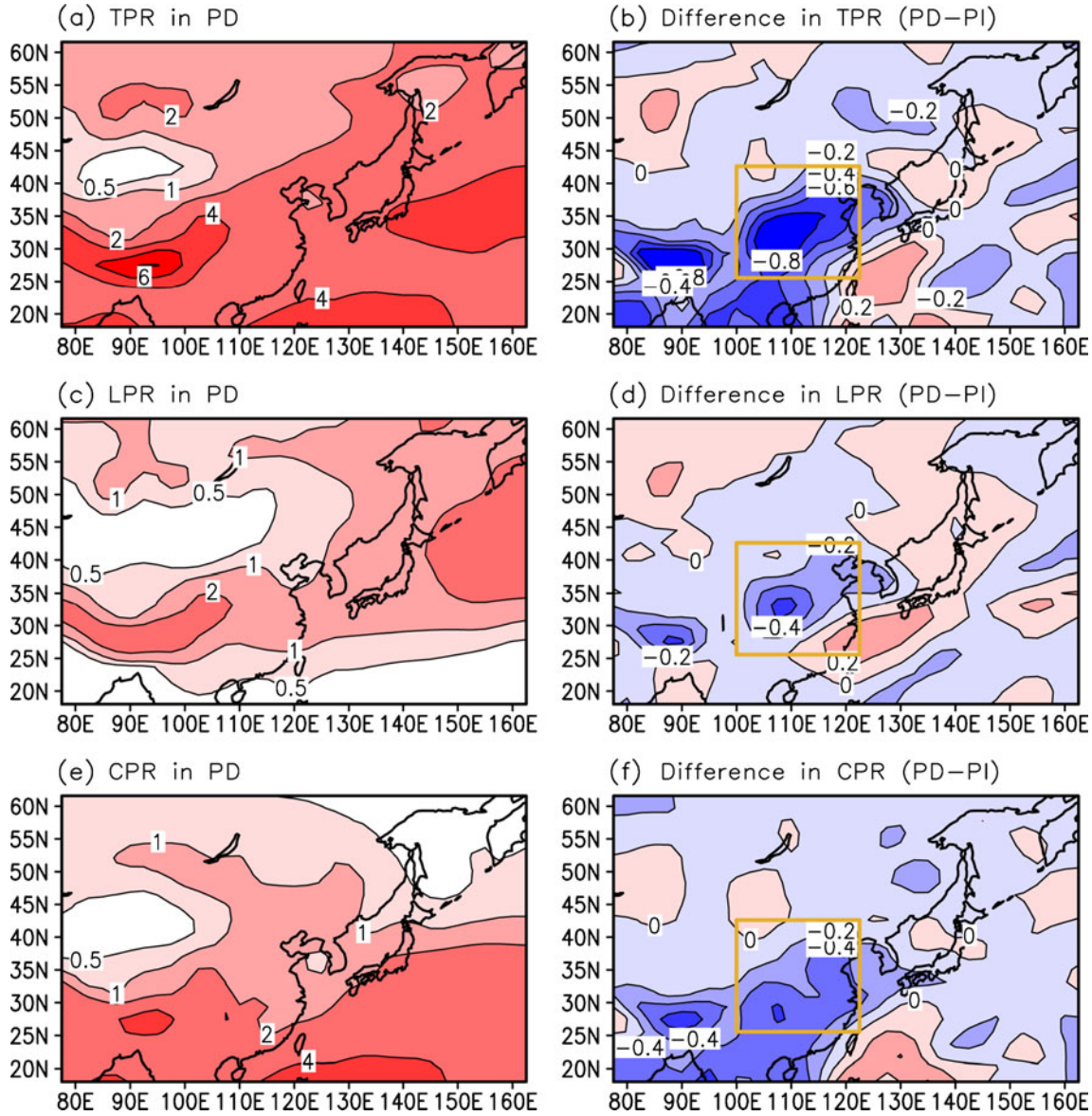


**Fig. 2** Spatial distributions of annual mean total (**a**), large-scale (**c**) and convective (**e**) precipitation rate in the PD and the corresponding total (**b**), large-scale (**d**) and convective (**f**) precipitation rate difference between the PD and PI experiment. The *yellow rectangle* labels the area of East China. Unit: mm/day

**Table 1** Seasonal and annual mean total precipitation, large-scale precipitation and convective precipitation rates (mm/day) in the PD and PI experiments, and their variations averaged for East Asia

| | Total precipitation | | | Large-scale precipitation | | | Convective precipitation | | |
|---|---|---|---|---|---|---|---|---|---|
| | PD | PI | (PD–PI)/PI (%) | PD | PI | (PD–PI)/PI (%) | PD | PI | (PD–PI)/PI (%) |
| Spring | 2.45 | 2.65 | −7.5 | 1.18 | 1.24 | −4.8 | 1.27 | 1.42 | −10.6 |
| Summer | 4.50 | 4.97 | −9.5 | 0.98 | 1.08 | −9.3 | 3.52 | 3.89 | −9.5 |
| Autumn | 3.00 | 3.04 | −1.3 | 1.11 | 1.13 | −1.8 | 1.89 | 1.91 | −1.0 |
| Winter | 1.72 | 1.70 | 1.2 | 0.99 | 0.97 | 2.1 | 0.73 | 0.73 | 0.0 |
| Annual | 2.92 | 3.09 | −5.8 | 1.07 | 1.11 | −3.6 | 1.87 | 2.00 | −6.5 |

indicated that the increased black carbon aerosols may increase the precipitation in certain areas in East Asia, e.g., the middle and lower reaches of the Yangtze River (Menon et al. 2002) and Northwest China (Gu et al. 2010), our results suggest that precipitation over East Asia generally decreases with the increase in aerosols when both the aerosol's direct and indirect effects are considered.

### 3.2 Effects of aerosols on cloud microphysical properties

A comparison between the spatial patterns of the changes in the annual mean precipitation rates (Fig. 2b) and AOD (Fig. 1e) indicates that the reduced precipitation and increased AOD in East China have a strong corresponding relationship. This negative correlation is further revealed by the fitted curve in the scatterplot of precipitation amount versus AOD (Fig. 3). The significant correspondence between precipitation change and AOD increment is indicative of the indirect aerosol effects on precipitation by influencing the cloud microphysical properties. In order to investigate the relationships between aerosols and cloud microphysical properties, we compare the annual mean values of AOD, precipitation rate, and various cloud microphysical properties over East China in the PI and PD experiments (Table 2). The results show that the column cloud droplet number concentration (DNC) and cloud liquid water path have increased by 137% and 28%, respectively, with the increase in atmosphere aerosols, while the cloud droplet effective radius (DER) has decreased by 20%. Furthermore, the probability distribution function of DER in both East Asia (Fig. 4a) and East China (Fig. 4b) indicates that the cloud droplets smaller (greater) than the DER of 8–10 μm occupy more (fewer) model grids in the PD experiment as compared to those in the PI experiment. In other words, the number of larger cloud droplets has been

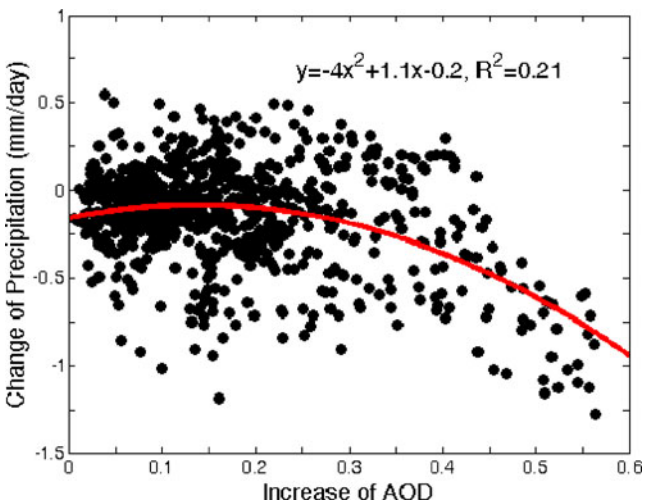


**Fig. 3** Scatterplots of precipitation change versus AOD increase between the PD and PI experiments. The overlaid is the least-squared fit

**Table 2** The annual-mean AOD, cloud microphysical properties, cloud amount, precipitation rates in the PD and PI experiments, and their corresponding variations over East China

| Experiment | PD | PI | (PD–PI)/PI (%) |
|---|---|---|---|
| AOD | 0.40 | 0.16 | 150 |
| DNC ($10^6$ cm$^{-2}$) | 5.66 | 2.39 | 137 |
| LWP (g cm$^{-2}$) | 91.4 | 71.2 | 28 |
| DER (μm) | 9.0 | 11.2 | −20 |
| High cloud cover (%) | 31.6 | 32.9 | −4.0 |
| Middle cloud cover (%) | 28.0 | 28.5 | −1.8 |
| Low cloud cover (%) | 24.1 | 25.3 | −4.7 |
| Total cloud cover (%) | 47.9 | 49.4 | −3.0 |
| Large-scale rainfall (mm/day) | 1.21 | 1.34 | −9.7 |
| Convective rainfall (mm/day) | 1.68 | 2.00 | −16 |
| Total precipitation (mm/day) | 2.89 | 3.34 | −13 |

reduced in the PD experiment, whereas the number of smaller cloud droplets has increased when compared to those in the PI experiment. Additionally, the PD–PI differences in the DER size distribution in East China (Fig. 4b) are greater than those in East Asia (Fig. 4a) as the former contains the main sources of aerosol emissions. The reverse pattern of the PD–PI cloud droplets smaller and larger than 8–10 μm suggests that the precipitation efficiency is reduced in the PD experiment as compared to that in PI. In other words, the changes in cloud microphysical properties lead to less precipitation in the PD simulation. For the changes in the precipitation rates in East China, the large scale and convective precipitation rates are reduced by 9.7% and

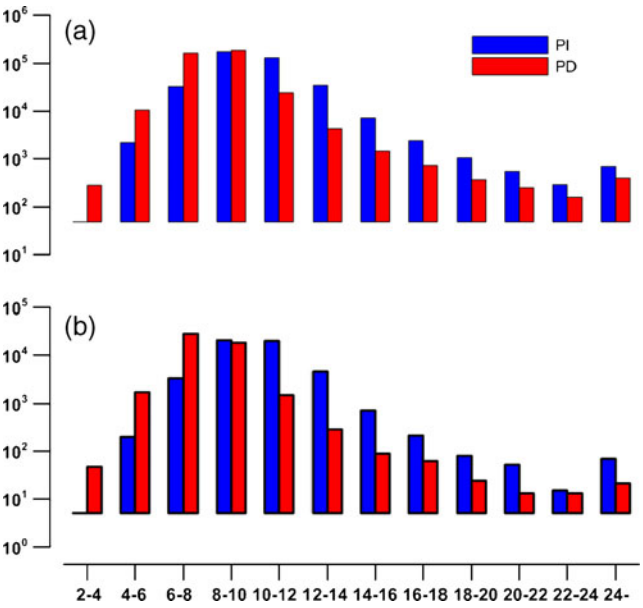


**Fig. 4** Size distribution on DER in both East Asia (**a**) and East China (**b**), *x*-axis labels the range of DER (μm), *y*-axis labels the total number of grid points with the corresponding DER. Note that each point represents monthly means in every grid

16%, respectively, and the total precipitation rate is reduced by 13% corresponding to the increased aerosols (Table 2). Based on the interactions between aerosols and cloud microphysical properties, the enhanced activation of aerosols in the PD experiment forms more cloud droplets with higher DNC values but smaller effective radius, which leads to less effective droplet coalescence and hinders the conversion of cloud droplets to raindrops. This result conforms with theories and observations regarding the second indirect effect of the aerosols acting as the cloud condensation nuclei (Albrecht 1989; Breon et al. 2002).

It should be pointed out that, however, the microphysics in CAM 3.5 is only for stratiform (grid scale) clouds and precipitation, and the aerosol impacts on subgrid-scale convective nucleation are not included in the employed cumulus parameterization scheme. Therefore, the significant changes in convective precipitation should result from other physical causes. The responsible mechanism is likely related to the radiatively induced atmospheric stabilization by the aerosol direct and indirect effects as evidenced in the vertical temperature structure differences (Fig. 5). Apparently, the tropospheric atmosphere is stabilized by the radiative effects of aerosols that cool the surface and warm the upper troposphere (the "semi-direct" effect). In particular, the static stability in the layer between the surface and 750 hPa is enhanced by approximately 5%, and this aerosol-induced lower-level stabilization is certainly detrimental to convective initiation and development. To fully understand and quantify the influences of the aerosol-induced atmospheric stability and other physical processes on convective precipitation, further investigations using diagnostic analyses and sensitivity experiments are needed.

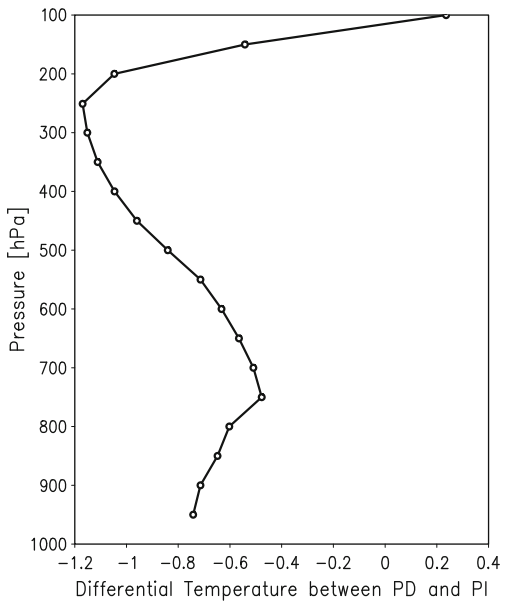


**Fig. 5** Vertical profile of differential summer temperature (°C) between the PD and PI experiments (PD–PI) over East China

Compared to the changes in cloud microphysical properties and precipitation rate, the annual mean values of cloud amount of high, middle, and low clouds have relatively minor reductions in East China (Table 2). The cloudiness decrease seems inconsistent with the second aerosol indirect effect. This is likely related to various aerosol-induced feedbacks in radiation thermodynamics and monsoon dynamics. Further discussions are presented in Section 4. Because summer precipitation is predominant in the annual amount across the East Asia monsoon region, it is also affected most effectively by the aerosols, corresponding to the greatest increases in aerosol concentrations among the four seasons (Fig. 1). In the following, we will investigate the changes in large-scale circulation patterns to reveal the effects of the increased aerosols on the East Asian summer monsoon circulation and the associated changes in precipitation.

## 3.3 Effects of aerosols on East Asian monsoon

### *3.3.1 Summer monsoon circulation*

With the prevailing summer monsoon systems across Asia, the southwesterly monsoonal winds dominate South Asia in the lower troposphere, while the southerly monsoonal winds dominate East Asia in the PD experiment (Fig. 6a). Figure 6b displays the PD–PI differences between the summer 850 hPa wind fields. With increasing aerosols in the PD experiment, the Asian summer monsoons have been weakened remarkably. For example, the westerly monsoonal winds over South Asia and the southerly monsoonal winds in South China are both weakened; while the tendency of forming anti-cyclonic circulation patterns in the low-elevation region in East China east of the Tibetan Plateau is enhanced. Hence, one can see that the net effect of the increased aerosols is to reduce the intensity of the Asian summer monsoon systems.

The weakened East Asian summer monsoon leads to the reductions in the northward water vapor transport and the upward air movement in the middle troposphere (500 hPa; figures are not shown). The average values of the 850 hPa meridional wind velocity, the 850 hPa meridional moisture flux, and the 500 hPa vertical upward velocity (negative as upward) are reduced by 14.3%, 16.0%, and 14.3% in the PD experiment, respectively; while the changes in the 850 hPa specific humidity and the precipitable water are relatively small in East Asia (Table 3). These results suggest that, associated with the weakened summer monsoon intensity, the net effect of aerosols is to suppress convection activities through the aerosol radiative stabilization mechanism discussed above, and thus to reduce the monsoonal precipitation in East Asia. Since the thermodynamic contrast between landmass and ocean is considered

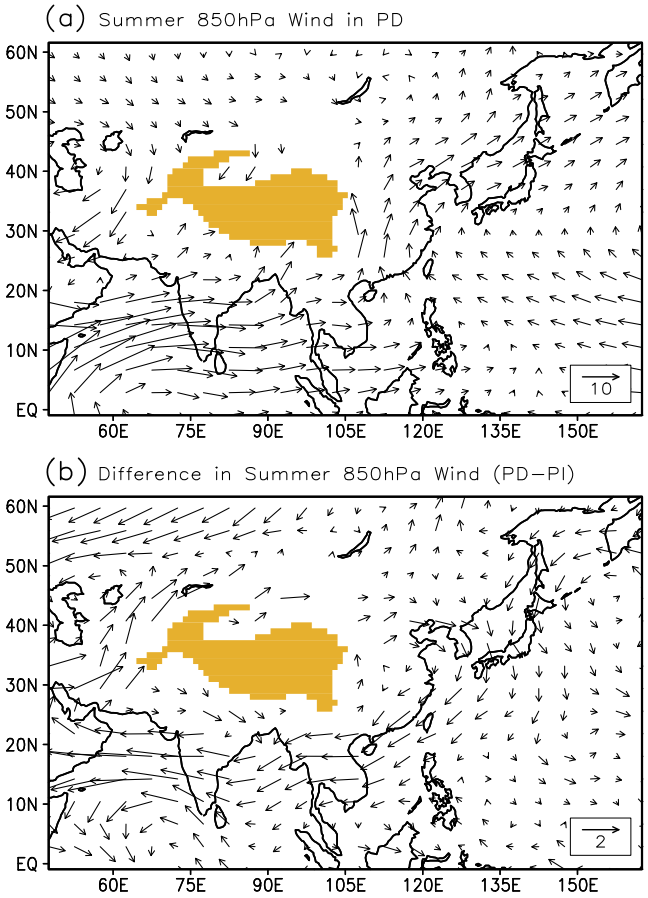


**Fig. 6** Spatial distributions of the summer-averaged Asian 850 hPa wind field in the PD (**a**) and the corresponding wind field difference between the PD and PI experiment (**b**). The *yellow shaded area* indicates the plateau above 2,000 m

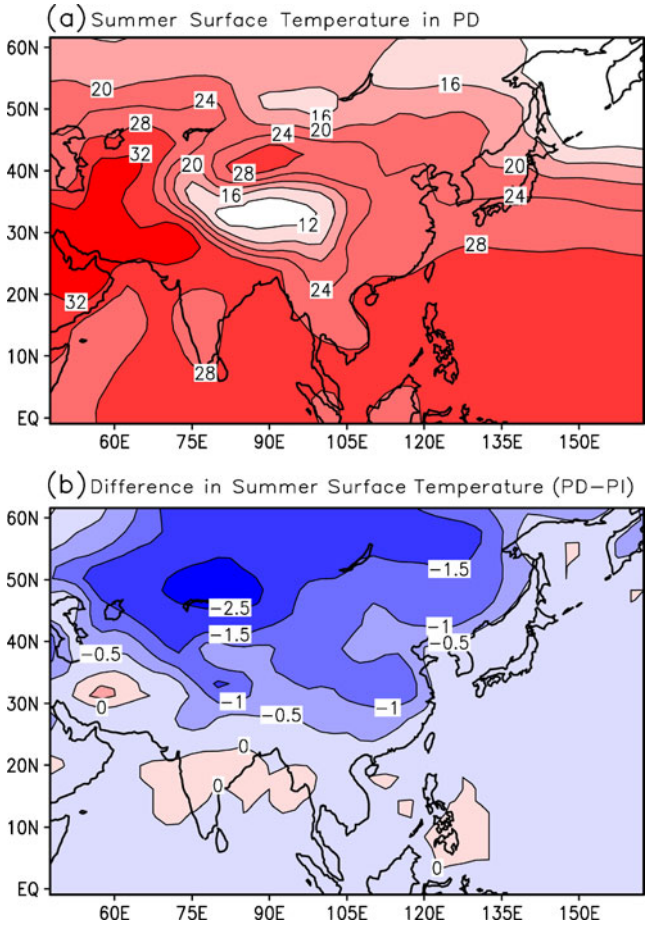


**Fig. 7** Same as Fig. 2 but for the summer–mean surface air temperature (°C)

as the main driving mechanism of the East Asian monsoon circulation (Webster 1987), it is necessary to examine the changes in surface air temperatures in East Asia associated with the aerosol concentrations.

### *3.3.2 Surface air temperature and ocean–land thermodynamic contrast*

Figure 7a shows the simulated summer surface air temperature field in East Asia in the PD experiment, which conforms well to the observations, with the main characteristics of decreasing temperatures from south to north and low temperatures centered at the Tibetan Plateau. Although a significant global temperature rise has been observed since the Industrial Revolution (IPCC 2007), the surface air temperature would have been significantly reduced if only considering the changes in aerosols in East Asia as shown by the PD–PI temperature differences in Fig. 7b. Increased aerosol concentrations lead to decreases in surface air temperature, with the area of the largest temperature decrease (beyond −2.5°C) near the Lake Balkhash. On the other hand, the differences in temperatures over the ocean between the PD and PI experiments are very small because the same SST boundary condition is used in both experiments and the changes in aerosols mainly occur over the land.

**Table 3** The 850 hPa meridional velocity, 850 hPa meridianal moisture flux, 850 hPa specific humidity, precipitable water, and 500 hPa vertical velocity averaged for summer over East China in the PD and PI experiments and their differences

| Experiment | PD | PI | (PD–PI)/PI (%) |
|---|---|---|---|
| Meridional velocity (m/s) | 1.68 | 1.96 | −14.3 |
| Meridional moisture flux (g m/kg/s) | 19.9 | 23.7 | −16.0 |
| Specific humidity (g/kg) | 10.2 | 10.5 | −2.9 |
| Precipitable water (kg/m$^2$) | 36.1 | 37.7 | −4.2 |
| Vertical velocity (Pa/s) | −0.0197 | −0.0230 | −14.3 |

Previous modeling studies that only considered the direct effects on radiative forcing of the aerosols concluded that the increased aerosol concentrations can cause surface cooling across the Asian continent (e.g., Giorgi et al. 2002), while in our study, the cooling effects of the aerosols are more prominent, as shown in Figs. 5 and 7, since both the direct and indirect effects of the aerosols are included. Such a spatial pattern of temperature changes, with cooling land surface temperatures and essentially unchanged SST, should decrease the thermodynamic contrast between ocean and land leading to the weakening of the Asian summer monsoons.

It is noticed that the basic spatial pattern, especially the land–sea contrast, in the PD–PI temperature difference is persistent throughout the troposphere characterized by moderate cooling over the land and minimal cooling or warming over the ocean (not shown). Consequently, even though the surface temperature change is rather weak over the Indian Subcontinent (Fig. 7b), the integrated cooling impact throughout the troposphere on the lower-level pressure field is significant enough to account for the weakened westerly monsoonal flows in South Asia.

### 3.3.3 Radiative forcing of the aerosols

The surface cooling caused by the increased aerosols is achieved through the aerosol total radiative forcing including the direct and indirect effects of the aerosols. Table 4 compares the top of atmosphere (TOA) and surface net shortwave, net longwave, and net total radiative fluxes between the PD and PI experiments at the global and regional scales. It is clear that the changes in net total radiation, at both TOA and surface, are mainly caused by the changes in shortwave radiation. For example, the change in the total net radiative flux at the surface in East Asia is −9.4 W/m$^2$ in the PD as compared to the PI level, corresponding to the change in the net shortwave radiative flux at the surface of −9.8 W/m$^2$, while the change in the net longwave radiative flux at the surface is only 0.4 W/m$^2$. Hence, one can see that the aerosol total radiative forcing affects the earth's surface energy balance mainly by reducing the net shortwave radiative flux.

Figure 8 shows the spatial distribution of the aerosol shortwave radiative forcing at the surface, the area beyond the value of −20 W/m$^2$ is located in the region from the Shandong Peninsula of China to the Korean Peninsula, which is similar as the area of increased aerosols (Fig. 1b). The aerosol radiative forcing makes the thermodynamic contrast between the land and sea decrease. It is interesting to note the different spatial patterns of the changes in surface air temperatures (Fig. 7) and radiative forcing (Fig. 8). The area of the largest cooling due to increased aerosol concentrations does not match that of the greatest reduction in radiative forcing. That is because, at the regional scale, the temperature distribution pattern and its responses to radiative forcing are affected by complex surface and atmospheric processes. The interactions between moisture conditions, hydrologic cycle, especially the latent heat flux, and circulation patterns play important roles in determining the eventual spatial pattern of surface temperatures on the Asian continent and its corresponding changes. To determine the complex interactions between the aforementioned physical processes that cause the spatial pattern of the temperature changes, however, further sensitivity studies are needed for a conclusive cause attribution in the future.

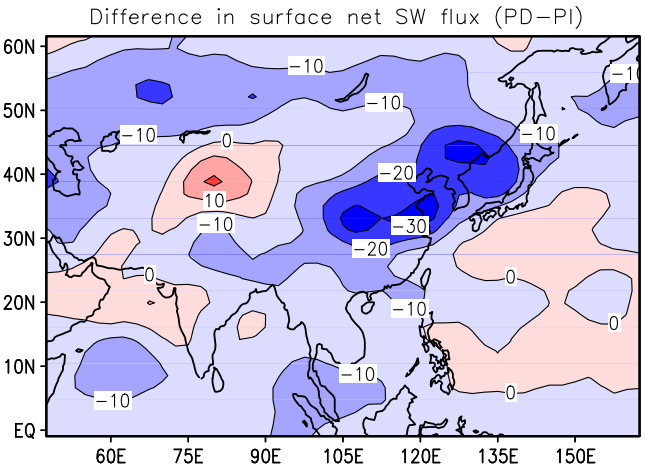


**Fig. 8** Spatial distribution of the net shortwave radiative flux difference between the PD and PI experiment at the surface. Unit: W/m$^2$

## 4 Conclusion and discussions

In this study, we have used the NCAR CAM Model (version 3.5) coupled with the Morrison–Gettelman two-

**Table 4** Changes (PD–PI) of net shortwave (SW), net longwave (LW), and net total radiative fluxes at the surface and at the top of atmosphere (TOA) for global and regional averages

| Variables | | Global | East Asia (land) | East China (land) |
|---|---|---|---|---|
| TOA | Net SW radiation | −2.9 | −8.6 | −13.8 |
| | Net LW radiation | 0.7 | 1.8 | 2.4 |
| | Net radiation | −2.2 | −6.8 | −11.4 |
| Surface | Net SW radiation | −3.7 | −9.8 | −19.2 |
| | Net LW radiation | −0.2 | 0.4 | 2.5 |
| | Net radiation | −3.9 | −9.4 | −16.7 |

Down is positive. Unit: W/m$^2$

moment cloud microphysics scheme to simulate the aerosol effects on clouds and precipitation for the years 2000 (PD experiment) and 1750 (PI experiment) in East Asia, where anthropogenic aerosols have increased dramatically during the past decades. We attempt to isolate the climate effects of aerosols by using the same set of boundary conditions in both experiments. As our experiments consider both the direct and indirect aerosol effects, the results offer a more complete insight into the climatic effects of the aerosols than many previous modeling studies. Our results indicate that the increase in aerosol concentrations represented by AOD is mainly in the region from the lower reach of the Yangtze River to North China in eastern China, expanding toward northeast to Korea and Japan. The peak increased in AOD in the PD experiment from the PI levels can reach 0.7 and higher from spring to fall with the greatest increases occurring in summer coinciding with the peak monsoon season. The cloud microphysical properties are markedly affected by the increase in aerosols from the PI levels, with increasing cloud droplet number concentration and liquid water path, but decreasing droplet effective radius, clearly illustrating the aerosol's second indirect effect on stratiform clouds. Under the condition of relatively stable atmospheric moisture flux, the enhanced cloud droplet number concentration with smaller droplet size will hinder the coalescence and conversion of cloud droplets to raindrops and subsequently reduce precipitation across East China, where we have seen the greatest increases in aerosols.

Besides the aerosol second indirect effect, some other mechanisms related to increased aerosols have also been proposed to be responsible for the reduced precipitation over East Asia. The aerosol-induced differential cooling between the surface and upper levels acts to stabilize the atmosphere, particularly the lower-level troposphere from the surface to 750 hPa, and thus leads to the suppression of convective activity. On the other hand, increased aerosol concentrations can cause spatially differential cooling, especially affecting the land–sea contrasting temperature variations, by modulating radiative forcing through the direct aerosol effect (e.g., Giorgi et al. 2002) and the first indirect effect (e.g., Penner et al. 2004). The changes in the radiation balance at the top of atmosphere and on surface due to increased aerosol concentrations are mostly determined by the aerosol radiative forcing on the shortwave radiation fluxes over the East Asia landmass, which leads to the cooling of the land surface across East Asia in the PD experiment. As a result, the thermodynamic differentiation between the Asian landmass and the surrounding oceans is reduced. Such reduced land–sea thermodynamic contrast will weaken the intensity of the Asian monsoon systems, as reflected in the reduced monsoonal wind velocities and moisture fluxes at the 850 hPa level, and mid-tropospheric vertical air movement or convective activity. The weakened Asian monsoon systems not only contribute to the overall reduction in summer precipitation, but also to the anomalous pattern of "north drought with south flooding" in East China as observed in recent decades.

Compared to the associations between aerosol concentrations and precipitation regimes revealed by observational studies (Zhao et al. 2006; Duan and Mao 2009), our numerical experiments have successfully explained the physical mechanisms associated with the increase in aerosol concentrations as one of the important causes for the reduction in precipitation in East Asia. However, further studies are still necessary to better distinguish the effects of all involved physical processes, especially those of the atmosphere dynamics. The variation in monsoon precipitation depends on not only the changes in cloud microphysical properties induced by aerosols, but also the associated changes in the monsoon circulation dynamics. What we have found in East Asia should also be applicable in other monsoon regions, such as South Asia and Northeast Africa (Sud et al. 2009). In this study, we specifically investigated the aerosol effects by our design of experiments, while the effects of the anthropogenic greenhouse gasses (IPCC 2007) and the large-scale atmosphere–ocean interactions (Zhou et al. 2008) must all be considered to determine the actual climate change since the Industrial Revolution. Our experiments indicate that increased aerosols in East Asia will weaken the intensity of the East Asian summer monsoon, which in turn will reduce summer precipitation in the region. Based on an index for the East Asian summer monsoon intensity calculated by Guo (1983), it was found that precipitation in North and Northeast China is positively correlated to the monsoon intensity, while precipitation in South China has an opposite tendency. On the other hand, precipitation in the lower reach of the Yangtze River of central eastern China tends to have above-normal precipitation with the normal monsoon intensity, but below-normal precipitation occurs in both strong and weak monsoon years. With the weakened East Asian summer monsoon, the conditions of normal and below-normal monsoon intensities become more frequent, which lead to reduced precipitation in eastern China in general, with more drought occurrences in North China, but the lower reach of the Yangtze River should experience enhanced variability with both droughts and flooding conditions. Other studies also pointed out that during the years with intensified East Asian summer monsoon, the monsoon rain belt can proceed further north and west in China (e.g., Ding and Wang 2008). Nevertheless, the pattern of "north drought with south flooding" in East China cannot be entirely attributed to the increases in aerosol concentrations (Hu et al. 2003; Qian et al. 2007). For example, the reduced precipitation in South China may be caused by the combined effects of the tropical ocean SST forcing, increased aerosols, and anthro-

pogenic greenhouse gasses, while the increase in precipitation in the Yangtze River Basin may not be related to aerosols at all (Cheng et al. 2005).

Many phenomena revealed by this paper deserve further in-depth studies using diagnostic analyses and sensitivity simulations. For example, the causes for the reduced convective precipitation, other than the enhanced atmospheric stability due to the radiative forcing of aerosols, need further investigation. In addition, we do not fully understand why the spatial pattern of surface temperature changes mismatches that of aerosol loading. In our experiments, we only considered the aerosols acting as cloud condensation nuclei in warm clouds and precipitation processes. The aerosol effects on ice nucleation are not represented in this model, which can be an important process related to the development of deep convective clouds as a major mode of summer precipitation. Therefore, further studies including the impacts of aerosols on activations of both cloud droplets and ice particles and the associated large-scale atmospheric dynamics are necessary to fully understand the aerosol effects on clouds and precipitation over East Asia, especially North China. Additionally, the simulated time interval is relatively short in this study, which limits the feasibility of using more sophisticated statistical methods to analyze the results.

**Acknowledgments** This work was supported by China Special Fund for Nonprofit Organizations (GYHY200706036), National Basic Research Program of China (2011CB403406), CAS Science and Technology Specific Project (XDA05110101) and NSFC (40825008).

## References

Albrecht BA (1989) Aerosols, cloud microphysics, and fractional cloudiness. Science 245:1227–1230

Breon FM, Tanre D, Generoso S (2002) Aerosol effect on cloud droplet size monitored from satellite. Science 295:834–838

Cheng YJ, Lohmann U, Zhang JH, Luo YF, Liu ZT, Lesins G (2005) Contribution of changes in sea surface temperature and aerosol loading to the decreasing precipitation trend in southern China. J Climate 18:1381–1390

Collins WD, Rasch PJ, Boville BA, Hack JJ, McCaa JR, Williamson DL, Kiehl JT, Briegleb B, Bitz C, Lin SJ, Zhang M, Dai Y (2004) Description of the NCAR Community Atmosphere Model (CAM 3.0). NCAR Tech. Note NCAR/TN-464+STR, 226 pp

Dentener F, Kinne S, Bond T, Boucher O, Cofala J, Generoso S, Ginoux P, Gong S, Hoelzemann JJ, Ito A, Marelli L, Penner JE, Putaud J-P, Textor C, Schulz M, van der Werf GR, Wilson J (2006) Emissions of primary aerosol and precursor gases in the years 2000 and 1750 prescribed data-sets for AeroCom. Atmos Chem Phys 6:4321–4344, http://www.atmos-chem-phys.net/6/4321/2006/

Ding YH, Wang ZY (2008) A study of rainy seasons in China. Meteorol Atmos Phys 100:121–138

Ding YH, Sun Y, Wang ZY, Zhu YX, Song YF (2009) Inter-decadal variation of the summer precipitation in China and its association with decreasing Asian summer monsoon Part II: possible causes. Intern J Climatol 29:1926–1944

Duan J, Mao JT (2009) Influence of aerosol on regional precipitation in North China. Chin Sci Bull 54:474–483

Emmons LK, Walters S, Hess PG, Lamarque JF, Pfister GG, Fillmore D, Granier C, Guenther A, Kinnison D, Laepple T, Orlando J, Tie X, Tyndall G, Wiedinmyer C, Baughcum SL, Kloster S (2010) Description and evaluation of the Model for Ozone and Related Chemical Tracers, version 4 (MOZART-4). Geosci Model Dev 3:43–67

Fu CB, Ma ZG (2008) Global change and regional aridification. Chin J Atmos Sci 32:752–760 (in Chinese)

Gent P, Bader D, Bonan G et al. (2009) Community Earth System Model Science Plan: 2009–2015. Available from http://www.ccsm.ucar.edu

Gettelman A, Morrison H (2008) A new two-moment bulk stratiform cloud microphysics scheme in the community atmosphere model, Version 3 (CAM3). Part II: single-column and global results. J Climate 21:3660–3679

Giorgi F, Bi X, Qian Y (2002) Direct radiative forcing and regional climatic effects of anthropogenic aerosols over East Asia: a regional coupled climate-chemistry/aerosol model study. J Geophys Res 107(D20):4439. doi:10.1029/2001JD001066

Giorgi F, Bi X, Qian Y (2003) Indirect vs. direct climatic effects of anthropogenic sulfate over East Asia as simulated with a regional coupled climate-chemistry/aerosol model. Clim Change 58:345–376

Gu Y, Liou KN, Xue Y, Mechoso CR, Li W, Luo Y (2006) Climatic effects of different aerosol types in China simulated by the UCLA general circulation model. J Geophys Res 111:D15201. doi:10.1029/2005JD006312

Gu Y, Liou KN, Chen W, Liao H (2010) Direct climate effect of black carbon in China and its impact on dust storms. J Geophys Res 115:D00K14. doi:10.1029/2009JD013427

Guo QY (1983) The summer monsoon intensity index in East Asia and its variation. Acta Ceographica Sinica 38:207–217 (in Chinese)

Hu ZZ, Yang S, Wu R (2003) Long-term climate variations in China and global warming signals. J Geophys Res 108(D19):4614. doi:10.1029/2003JD003651

Huang Y, Chameides WL, Dickinson RE (2007) Direct and indirect effects of anthropogenic aerosols on regional precipitation over east Asia. J Geophys Res 112:D03212. doi:10.1029/2006JD007114

Intergovernmental Panel on Climate Change (IPCC) (2007) Climate change 2007: the physical science Basis: Working Group I Contribution to the Fourth Assessment Report of the IPCC (AR4). WMO and UNEP. Cambridge University Press, Valencia, Spain

Khairoutdinov M, Kogan Y (2000) A new cloud physics parameterization in a large-eddy simulation model of marine stratocumulus. Mon Weather Rev 128:229–243

Kiehl JT, Gent PR (2004) The Community Climate System Model, version 2. J Climate 17:3666–3682

Kinne S et al (2006) An AeroCom initial assessment—optical properties in aerosol component modules of global models. Atmos Chem Phys 6:1815–1834

Lau KM, Kim KM (2006) Observational relationships between aerosol and Asian monsoon rainfall, and circulation. Geophys Res Lett 33:L21810. doi:10.1029/2006GL027546

Lau KM, Kim MK, Kim KM (2006) Asian summer monsoon anomalies induced by aerosol direct forcing: the role of the Tibetan Plateau. Climate Dyn 26:855–864

MA ZG (2007) The interdecadal trend and shift of dry/wet over the central part of North China and their relationship to the Pacific Decadal Oscillation (PDO). Chin Sci Bull 52:2130–2139

Massie ST, Torres O, Smith SJ (2004) Total Ozone Mapping Spectrometer (TOMS) observations of increases in Asian aerosol

in winter from 1979 to 2000. J Geophys Res 109:D18211. doi:10.1029/2004JD004620

Meehl GA, Arblaster JM, Collins WD (2008) Effects of black carbon aerosols on the Indian monsoon. J Climate 21:2869–2882

Menon S, Hansen J, Nazarenko L, Luo Y (2002) Climate effects of black carbon aerosols in China and India. Science 297:2250–2253

Morrison H, Gettelman A (2008) A new two-moment bulk stratiform cloud microphysics scheme in the community atmosphere model, Version 3 (CAM3). Part I: description and numerical tests. J Climate 21:3642–3659

Penner JE, Dong XQ, Chen Y (2004) Observational evidence of a change in radiative forcing due to the indirect aerosol effect. Nature 427:231–234

Qian Y, Leung LR, Ghan SJ, Giorgi F (2003) Regional climate effects of aerosols over China: modeling and observation. Tellus Ser B 55:914–934

Qian WH, Lin X, Zhu YF, Xu Y, Fu JL (2007) Climatic regime shift and decadal anomalous events in China. Clim Change 84:167–189

Qian Y, Gong D, Fan J, Leung LR, Bennartz R, Chen D, Wang W (2009) Heavy pollution suppresses light rain in China: observations and modeling. J Geophys Res 114:D00K02. doi:10.1029/2008JD011575

Quaas J, Ming Y, Menon S et al (2009) Aerosol indirect effects—general circulation model intercomparison and evaluation with satellite data. Atmos Chem Phys 9:8697–8717

Ramanathan V, Crutzen PJ, Kiehl JT, Rosenfeld D (2001) Aerosol, climate and the hydrological cycle. Science 294:2119–2124

Ramanathan V, Chung C, Kim D, Bettge T, Buja L, Kiehl JT, Washington WM, Fu Q, Sikka DR, Wild M (2005) Atmospheric brown clouds: impacts on South Asian climate and hydrological cycle. Proc Natl Acad Sci USA 102:5326–5333

Ramanathan V, Ramana MV, Roberts G et al (2007) Warming trends in Asia amplified by brown cloud solar absorption. Nature 448:575–578

Remer LA, Kleidman RG, Levy RC et al. (2008) Global aerosol climatology from the MODIS satellite sensors. J Geophys Res 113(D14S07). DOI: 10.1029/2007JD009661

Rosenfeld D, Lohmann U, Raga GB et al (2008) Flood or drought: how do aerosols affect precipitation? Science 321:1309–1313

Sud YC, Wilcox E, Lau WKM, Walker GK, Liu XH, Nenes A, Lee D, Kim KM, Zhou Y, Bhattacharjee PS (2009) Sensitivity of boreal-summer circulation and precipitation to atmospheric aerosols in selected regions—part 1: Africa and India. Ann Geophys 27:3989–4007

Twomey S (1974) Pollution and the planetary albedo. Atmos Environ 8:1251–1256

Webster PJ (1987) The elementary monsoon. In: Fein JS, Stephens PL (eds) Monsoons. Wiley, New York, pp 3–32

Wu J, Fu CB, Xu YY, Tang JP, Han ZW, Zhang RJ (2009) Effects of total aerosol on temperature and precipitation in East Asia. Clim Res 40:75–87

Xu Q (2001) Abrupt change of the mid-summer climate in central East China by the influence of atmospheric pollution. Atmos Environ 35:5029–5040

Zhang H, Wang ZL, Guo PW, Wang ZZ (2009) A modeling study of the effects of direct radiative forcing due to carbonaceous aerosol on the climate in East Asia. Adv Atmos Sci 26:57–66

Zhao C, Tie X, Lin Y (2006) A possible positive feedback of reduction of precipitation and increase in aerosols over eastern central China. Geophys Res Lett 33:L11814. doi:10.1029/2006GL025959

Zhou TJ, Yu RC, Li HM, Wang B (2008) Ocean forcing to changes in global monsoon precipitation over the recent half-century. J Climate 21:3833–3852